Kinetic and Product Study of the Reactions of C(1 D) with CH 4 and C 2 H 6 at Low Temperature

Dianailys Nuñez-Reyes, Kevin Hickson

A Kinetic and Product Study of the Reactions of $C(^1D)$ with CH_4 and C_2H_6 at Low Temperature

Dianailys Nuñez-Reyes[†,‡] *and Kevin M. Hickson**[, †,‡]

[†] Université de Bordeaux, Institut des Sciences Moléculaires, F-33400 Talence, France

[‡] CNRS, Institut des Sciences Moléculaires, F-33400 Talence, France

AUTHOR INFORMATION

Corresponding Author

kevin.hickson@u-bordeaux.fr

Abstract

The reactions of atomic carbon in its first excited ^{1}D state with both CH_4 and C_2H_6 have been investigated using a continuous supersonic flow reactor over the 50–296 K temperature range. C(^{1}D) atoms were generated in-situ by the pulsed laser photolysis of CBr_4 at 266 nm. To follow the reaction kinetics, product H-atoms were detected by vacuum ultraviolet laser induced fluorescence at 121.567 nm. Absolute H-atom yields for both reactions were determined by comparison with the H-atom signal generated by the reference C(^{1}D) + H_2 reaction. While the rate constant for the C(^{1}D) + CH_4 reaction is in excellent agreement with earlier work at room temperature, this process displays a surprising reactivity increase below 100 K. In contrast, the reactivity of the C(^{1}D) + C_2H_6 system decreases as the temperature falls, obeying a capture type rate law. The H-atom product yields of the C(^{1}D) + CH_4 reaction agree with the results of earlier crossed beam experiments at higher collision energy. Although no previous data is available on the product channels of the C(^{1}D) + C_2H_6 reaction, comparison with earlier work involving the same singlet C_3H_6 potential energy surface allows us to draw conclusions from the measured H-atom yields.

1 Introduction

Carbon is one of the most common elements in the Universe, with a predicted abundance ratio of (3-4) × 10^{-4} with respect to hydrogen.[1] The reactions of ground state atomic carbon are important processes in combustion chemistry,[2] in the chemistry of planetary atmospheres[3] and in the interstellar medium (ISM).[4] While C(^{3}P) atoms react rapidly with unsaturated hydrocarbons such as C_2H_2, C_2H_4 and longer carbon chain species,[5-9] their reactivity with saturated hydrocarbons such as CH_4 and C_2H_6 as well as with H_2 is considerably lower. Indeed, the lowest energy pathway connecting reagents with products in the C(^{3}P) + CH_4 reaction is characterized by a barrier of 51 kJ mol^{-1},[10] whereas the C(^{3}P) + H_2 reaction itself is highly endothermic.[11] In contrast, excited state C(^{1}D) atoms are known to react readily with a wide range of species including saturated hydrocarbons C_2H_2,[8] C_2H_4,[12, 13] C_3H_6[13] by addition to the double bond as well as with H_2,[14-17] D_2[15, 16, 18] and CH_4 [12, 19] by insertion into H-H (D-D) or C-H bonds respectively. In common with C(^{3}P) reactions, such processes could play a role in the chemistry of planetary atmospheres and in limited regions of the ISM such as the dense gaseous envelopes surrounding young stellar objects.

While the reaction of C(^{1}D) with H_2 leads to CH($^2\Pi$) + H(^{2}S) as the exclusive products, the reaction of C(^{1}D) with CH_4 has several possible exothermic exit channels:

$$C(^1D) + CH_4 \rightarrow H_2(^1\Sigma_g^+) + C_2H_2(^1\Sigma_g^+) \quad \Delta H°_0 = -536.7 \text{ kJ mol}^{-1} \quad (1a)$$

$$\rightarrow H_2(^1\Sigma_g^+) + CCH_2(^1A_1) \quad \Delta H°_0 = -353.8 \text{ kJ mol}^{-1} \quad (1b)$$

$$\rightarrow H(^2S) + HCCH_2(^2A') \quad \Delta H°_0 = -250.8 \text{ kJ mol}^{-1} \quad (1c)$$

$$\rightarrow H(^2S) + CCH_3(^2A'') \quad \Delta H°_0 = -45.0 \text{ kJ mol}^{-1} \quad (1d)$$

$$\rightarrow CH(^2\Pi) + CH_3(^2A_2'') \quad \Delta H°_0 = -24.9 \text{ kJ mol}^{-1} \quad (1e)$$

The quoted reaction enthalpies are taken from the calculations of Leonori et al.[19] who performed a combined experimental and theoretical investigation of the dynamical aspects of this process. Reaction (1) is thought to occur through the initial formation of a singlet $HCCH_3$ intermediate ($^1HCCH_3$), 394.1 kJ mol^{-1} lower in energy than the reagents. This species can then evolve in

several different ways, notably involving isomerization to the global C_2H_4 (^1A_g) minimum (-706.4 kJ mol^{-1} with respect to the reagent level) and/or dissociation through pathways (1a) to (1c). The dissociation pathways (1d) and (1e) leading from $^1HCCH_3$ were considered to be unimportant, given the high energy of these channels with respect to the initially formed $^1HCCH_3$ intermediate and the other potential products. Leonori et al.[19] also highlighted the possible influence of intersystem crossing on the dynamics of the C(^{1}D) + CH_4 reaction. Indeed, their Rice-Ramsperger-Kassel-Marcus (RRKM) estimates of a very short lifetime for the $^1HCCH_3$ intermediate were not in agreement with their fits to the laboratory frame angular and time-of-flight distributions which required center-of-mass angular distributions coherent with the formation of a bound intermediate having a relatively long lifetime (comparable to its rotational period). They suggested that these differences could have been caused by coupling between triplet and singlet states in the vicinity of the $HCCH_3$ intermediate, with earlier RRKM calculations by Kim et al.[10] estimating a much longer lifetime for triplet methylcarbene ($^3HCCH_3$). Consequently, these inconsistencies might be explained if intersystem crossing plays an important role in the the C(^{1}D) + CH_4 system.

There is little or no information regarding the reaction of C(^{1}D) with C_2H_6 in the literature. Nevertheless, as this process occurs through the formation of a C_3H_6 intermediate, we can examine the results of related studies which sample the same regions of the potential energy surface (PES). In this instance, we can refer to previous work on unimolecular decomposition of propene (C_3H_6) in its singlet ground state[20, 21] and other bimolecular reactions over the same PES[22-24] to allow us to draw some conclusions on the preferred product channels of the C(^{1}D) + C_2H_6 reaction.

Aside from the fundamental interest of the study of reactivity of C(^{1}D) atoms, the reactions of C(^{1}D) with CH_4 and C_2H_6 could also play a role in the chemistry of planetary atmospheres such as Titan, a moon of Saturn with a dense atmosphere composed mainly of CH_4 and N_2 with

traces of other hydrocarbons including C_2H_6. Interestingly, modeling studies of Titan's atmosphere[25] predict that the mole fraction of $C_3(^1\Sigma_g^+)$ reaches values as high as 10^{-4} at altitudes around 800 km; a molecule which is photodissociated in the vacuum ultraviolet wavelength range to produce either $C(^3P) + C_2(a^3\Pi_u)$ or $C(^1D) + C_2(X^1\Sigma_g^+)$ as spin-allowed products.

Here, we report the results of an experimental investigation of the kinetics of the $C(^1D) + CH_4$ and $C(^1D) + C_2H_6$ reactions over the 50-296 K temperature range using a supersonic flow reactor coupled with pulsed laser photolysis and vacuum ultraviolet laser induced fluorescence detection. In addition, H-atom product yields were measured over the same temperature range to provide further insight into the overall reaction mechanisms for these processes. Sections 2 and 3 describe respectively the experimental methods used and the results obtained, while the results are discussed in section 4. Our conclusions are presented in section 5.

2 Experimental Method

A continuous supersonic flow apparatus was employed in the present measurements to generate cold flows with uniform temperature, density and velocity profiles through the use of Laval type axisymmetric nozzles. This technique has been described in detail in previous work[26, 27] so only details relevant to the current study will be outlined here. Only Laval nozzles employing argon as the carrier gas were used during this investigation as all of our nitrogen based nozzles resulted in the rapid loss of excited state carbon atoms through the $C(^1D) + N_2$ quenching reaction.[28] These argon based nozzles, whose flow characteristics can be found in Table 1 of Grondin et al., [29] allowed temperatures of 50 K, 75 K and 127 K to be attained. In addition, room temperature (296 K) measurements were performed without a Laval nozzle at lower flow velocities, thereby avoiding potential pressure gradients in the reactor.

$C(^1D)$ atoms were produced in situ within the supersonic flow by the pulsed multiphoton dissociation of precursor molecule tetrabromomethane (CBr_4) at 266 nm; a process which also

led to C(^{3}P) formation.[9, 30-33] Indeed, the major product of CBr_4 photolysis at 266 nm was found to be ground state atomic carbon with a measured relative yield of approximately 85 % with respect to excited state atomic carbon under similar experimental conditions.[30] A small concentration of CBr_4 vapour was introduced into the Laval nozzle reservoir by passing a secondary argon flow through solid CBr_4 held at a known fixed pressure and temperature. Its concentration was controlled by varying the secondary argon flow and/or the pressure in the vessel containing CBr_4, allowing us to estimate a maximum concentration of 2×10^{13} molecule cm^{-3} in the supersonic flow.

As we were unable to detect C(^{1}D) atoms directly in this study, due to the lack of allowed transitions from these excited state atoms in the appropriate wavelength range, product hydrogen atoms in the ground ^{2}S state were followed instead, through pulsed vacuum ultraviolet laser induced fluorescence (VUV LIF) at 121.567 nm. The procedure for generating tunable radiation around 121.6 nm and the optical system employed to collect the VUV fluorescence have already been described in detail in previous publications[9, 17, 18, 28, 30, 32, 33] and will not be repeated here. The solar blind photomultiplier tube used to detect VUV fluorescence was fed into a boxcar integrator for quantitative signal acquisition and processing.

The rare gases and reagent gases (Ar 99.999%, Kr 99.99%, CH_4 99.9995%, C_2H_6 99.5%) employed during the course of these experiments were used directly from cylinders. All flows were controlled by mass flow controllers which were calibrated using a pressure rise at constant volume method. Knowledge of the carrier gas and reactive gas flows allowed us to control precisely the reagent and precursor concentrations within the supersonic flow.

3 Results

Large excess concentrations of both CH_4 and C_2H_6 (with respect to $C(^1D)$ atoms) were used in all experiments so that the pseudo-first-order approximation could be applied. Under these conditions, two different types of experiments were performed.

In the first type of experiment, which allowed us to study the kinetics of the $C(^1D)$ + CH_4 and $C(^1D)$ + C_2H_6 reactions, the $H(^2S)$ fluorescence signal produced by these processes was recorded as a function of time between the photolysis and probe lasers. These curves could be reproduced using a functional fit of the form;

$$I_H = A\{exp(-k_{L(H)}t) - exp(-k't)\} \quad (2)$$

The first term in expression (2) represents the loss of atomic hydrogen with a first-order rate constant $k_{L(H)}$. This term is mostly due to diffusional loss of the H-atoms from the probe volume with values in the range 2000-5000 s^{-1}. $k' = k[X] + k_{L(C)}$, where k represents the second order rate constant for the $C(^1D)$ + X reaction with X = CH_4 or C_2H_6, $k_{L(C)}$ represents the first-order loss of $C(^1D)$ by other processes such as secondary reactions and diffusion, [X] is the CH_4 or C_2H_6 concentration, t is time and A is the signal amplitude. Two typical H-atom formation curves for the $C(^1D)$ + CH_4 reaction are displayed in Figure 1.

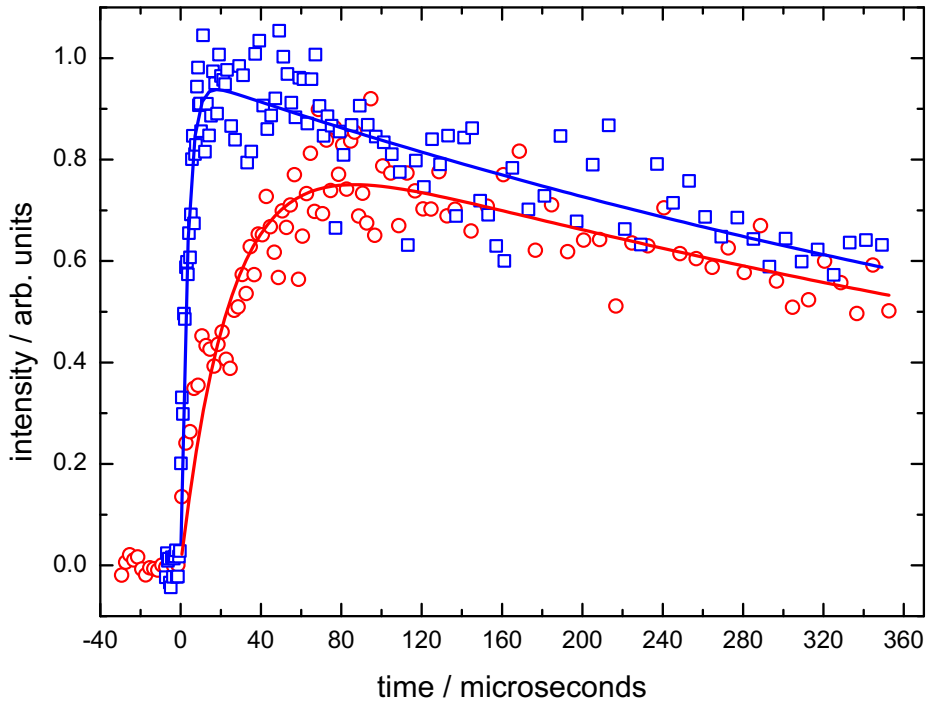

Figure 1 Measured product H-atom VUV LIF signal for the C(^{1}D) + CH_4 reaction as a function of time at 50 K. (Blue open squares) [CH_4] = 8.4 × 10^{14} cm^{-3}; (red open circles) [CH_4] = 8.7 × 10^{13} cm^{-3}.

These profiles were recorded at 50 K for C(^{1}D) in the presence of high (8.4 × 10^{14} cm^{-3}) and low (8.7 × 10^{13} cm^{-3}) concentrations of CH_4. H-atom profiles were recorded for several different alkane concentrations, yielding a wide range of values for the pseudo-first-order rate constant, k'. The second-order rate constant was obtained by plotting the k' values obtained at any specific temperature against the corresponding alkane concentration using a linear least-squares fitting method. Examples of such plots obtained at 50 K and at 296 K are shown in Figure 2 for both the C(^{1}D) + CH_4 and C(^{1}D) + C_2H_6 reactions. These fits were weighted using the statistical uncertainties generated by the biexponential fitting procedure outlined above, so that pseudo-first-order rate constants with higher uncertainty carried the least weight. The error bars on the measured second-order rate constants were derived by combining the statistical uncertainties of the second-order fits with an estimated 10 % systematic error. This systematic

error could have arisen from calibration errors in the various devices used to monitor and control the experiment such as mass-flow controllers and pressure gauges in addition to potential errors in the flow density and velocity calculations. Given the large concentration of $C(^3P)$ atoms present in the supersonic flow with respect to $C(^1D)$ atoms, it was important to check for the influence of secondary reactions which could eventually lead to supplementary hydrogen atom formation. The reaction of $C(^3P)$ with CH_4 is characterized by a large activation barrier of 51 kJ mol^{-1},[10] so that this reaction should be negligible at room temperature and below in the absence of tunneling effects. Nevertheless, a recent investigation of the $C(^3P)$ + H_2O reaction[32] clearly showed that despite the presence of a significant activation barrier (11-40 kJ mol^{-1}), reaction could still occur at low temperature through tunneling, leading to atomic hydrogen as one of the major products. In order to examine the potential for similar tunneling effects in the $C(^3P)$ + CH_4 reactions we performed additional test experiments at 50 K as shown in Figure S1 of the supporting information file. During these measurements, a large concentration of N_2 (3.2×10^{16} cm^{-3}) was added to the reactor, thereby rapidly quenching $C(^1D)$ atoms present in the supersonic flow.[28] Under these conditions, only small $H(^2S)$ fluorescence signals were recorded (eight times lower than the measured $H(^2S)$ signal in the absence of N_2), due to the reaction of some non-quenched $C(^1D)$ atoms with CH_4. It can be seen from Figure S1 that the variation of this $H(^2S)$ signal as a function of time yields time constants ($k' \approx 3.0 \times 10^5$ s^{-1}) for the rising part of the profile which are consistent with the rapid removal of $C(^1D)$ by N_2. Moreover, the long-time diffusion part of the H-atom profiles yields values for $k_{L(H)}$ which are essentially the same as those recorded in the absence of N_2, indicating that other slower H-atoms production pathways (such as those that would be expected if tunneling processes were important) are entirely negligible for this reaction.

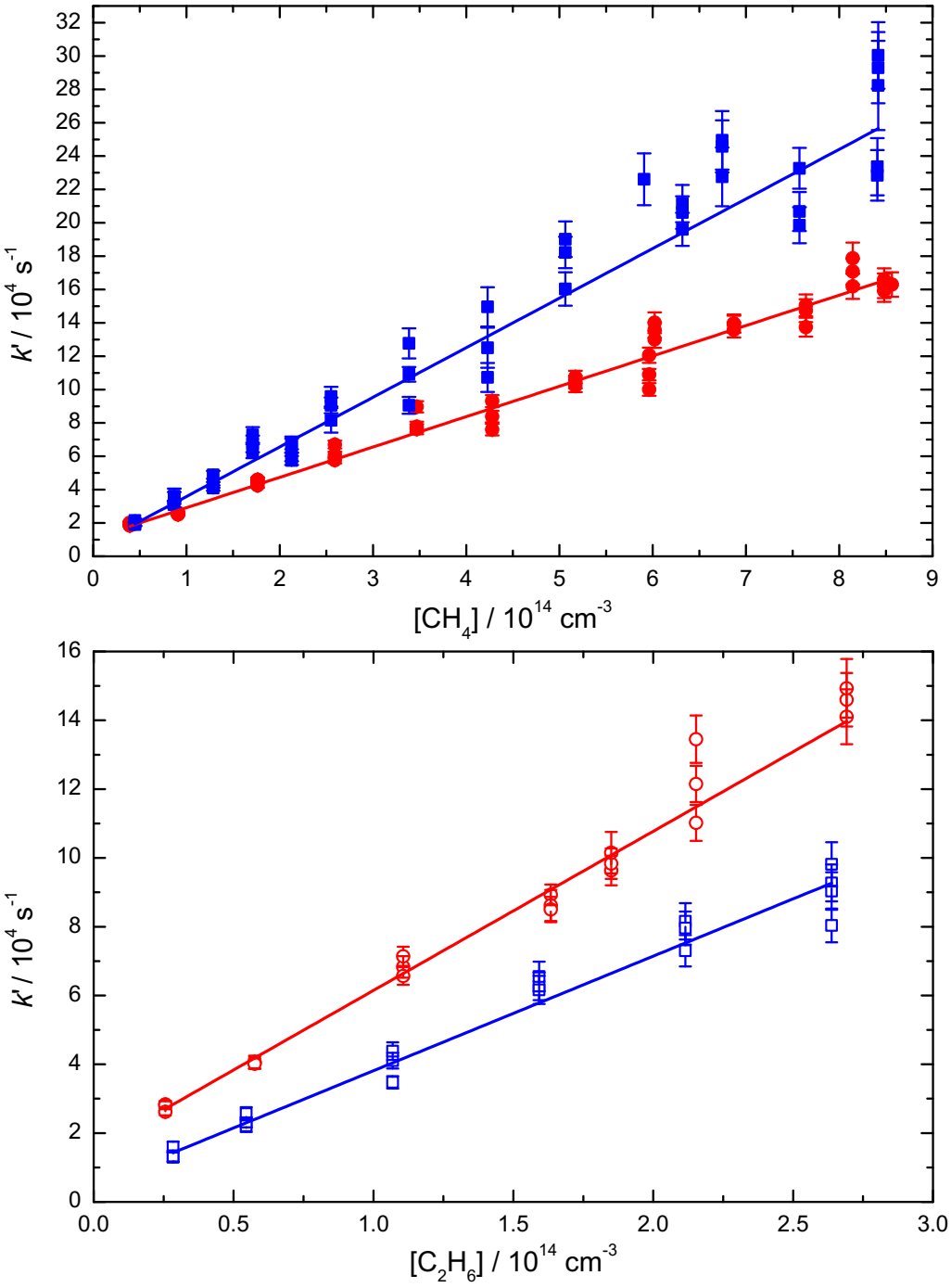

Figure 2 Second-order rate constants for the C(^{1}D) + alkane reactions. (Upper panel) The C(^{1}D) + CH_4 reaction at 50 K (blue solid squares) and at 296 K (red solid circles). (Lower panel) The C(^{1}D) + C_2H_6 reaction at 50 K (blue open squares) and at 296 K (red open circles). Solid lines

represent weighted fits to the individual datasets. Error bars represent the statistical uncertainties (1σ) derived from biexponential fits to temporal profiles such as those shown in Figure 1.

The measured rate constants for the $C(^1D) + CH_4$ and $C(^1D) + C_2H_6$ reactions are summarized in Table 1 and displayed as a function of temperature in Figure 3. While the rate constants for the $C(^1D) + CH_4$ reaction are seen to be large at all temperatures, we observe a surprising reactivity increase below 100 K, reaching a value of $(3.0 \pm 0.3) \times 10^{-10}$ cm^3 s^{-1} at 50 K; almost 70 % higher than the room temperature value. In contrast, the rate constants for the $C(^1D) + C_2H_6$ reaction increase with temperature reaching a value of $(4.6 \pm 0.5) \times 10^{-10}$ cm^3 s^{-1} at 296 K.

Table 1 Measured rate constants for the $C(^1D) + CH_4$ and $C(^1D) + C_2H_6$ reactions.

T / K	N[b]	$[CH_4]$ / 10^{14} cm^{-3}	$k_{C(1D)+CH4}$ / cm^3 s^{-1}	N	$[C_2H_6]$ / 10^{14} cm^{-3}	$k_{C(1D)+C2H6}$ / cm^3 s^{-1}
296	40	0.4-8.6	(1.8 ± 0.2)[c] $\times 10^{-10}$	21	0.3-2.2	$(4.6 \pm 0.5) \times 10^{-10}$
127±2[a]	59	0.7-12.3	$(1.9 \pm 0.2) \times 10^{-10}$	29	0.2-2.0	$(3.4 \pm 0.4) \times 10^{-10}$
75±2	42	0.6-6.0	$(2.3 \pm 0.3) \times 10^{-10}$	21	0.2-2.7	$(2.8 \pm 0.3) \times 10^{-10}$
50±1	44	0.4-8.4	$(3.0 \pm 0.3) \times 10^{-10}$	21	0.3-2.6	$(3.3 \pm 0.4) \times 10^{-10}$

[a]Uncertainties on the calculated temperatures represent the statistical (1σ) errors obtained from Pitot tube measurements of the impact pressure; [b]Number of individual measurements; [c]Uncertainties on the measured rate constants represent the combined statistical and systematic errors as explained in the text.

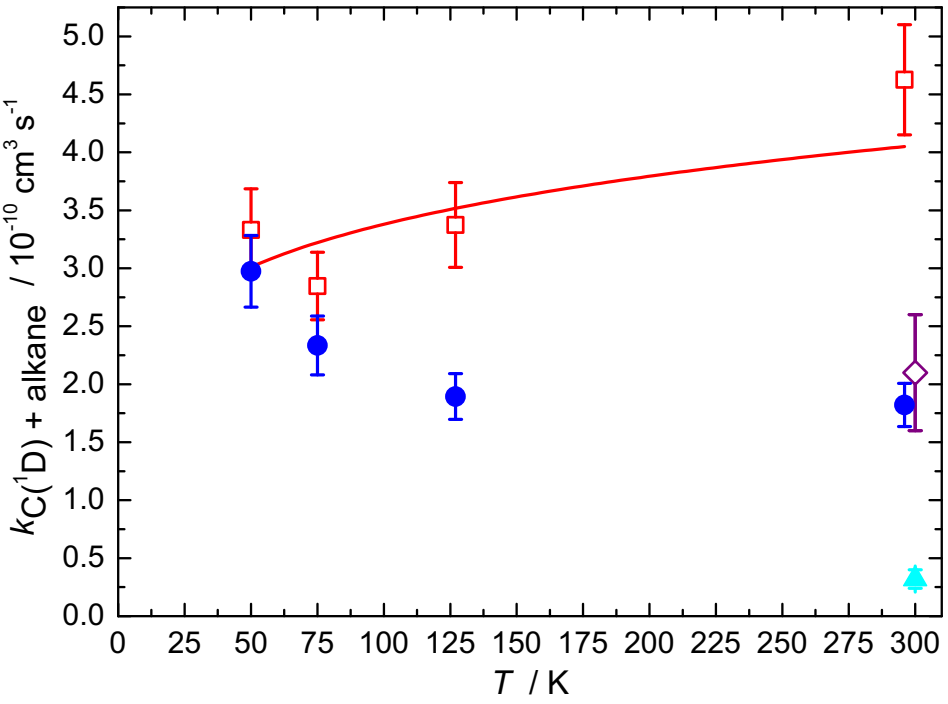

Figure 3 Second-order rate constants for the C(^{1}D) + alkane reactions as a function of temperature. The C(^{1}D) + CH_4 reaction: (blue solid circles) this work; (cyan solid triangle) Braun et al.[34]; (purple open diamond) Husain and Kirsch.[12] (Red open squares) the C(^{1}D) + C_2H_6 reaction. The red solid line represents the fit to the C(^{1}D) + C_2H_6 rate data with a fixed $T^{1/6}$ temperature dependence. Error bars represent the combined statistical and systematic uncertainties. Statistical uncertainties are derived from weighted linear least squares fits to plots of the first-order rates as a function of concentration (see Figure 2). The systematic uncertainty is estimated at the level of 10 % of the nominal rate constant (see text for more details).

In the second type of experiment, which allowed us to derive absolute H-atom product yields as a function of temperature, the time dependent H-atom signal intensities of the C(^{1}D) + CH_4 and C(^{1}D) + C_2H_6 reactions were compared to those obtained from a reference process, namely the C(^{1}D) + H_2 reaction with a known atomic hydrogen yield of 100 %.[17] To ensure that H-atom losses such as those described in expression (1) above did not lead to errors in the absolute yields, the alkane and H_2 concentrations were adjusted to obtain curves with similar values of k'. Several pairs of H-atom curves were recorded at each temperature to reduce uncertainties in

the absolute yields. Moreover, the order in which the curves were acquired was inverted on a regular basis to account for potential variations in the fluorescence intensities as a function of experiment time. A pair of H(^{2}S) temporal profiles recorded sequentially for the C(^{1}D) + CH_4 and C(^{1}D) + H_2 reactions at 50 K is shown in Figure 4.

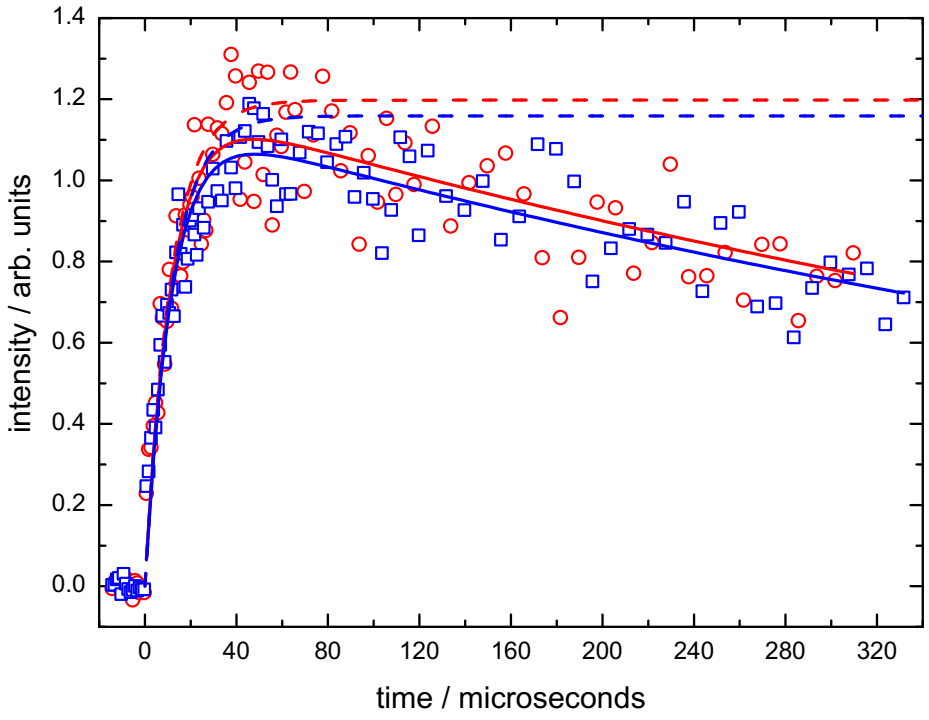

Figure 4 H-atom VUV LIF emission profiles recorded at 50 K. (Red open circles) H-atom signal from the C(^{1}D) + CH_4 reaction with [CH_4] = 2.1 × 10^{14} cm^{-3}; (red solid line) biexponential fit to the C(^{1}D) + CH_4 datapoints; (red dashed line) theoretical H-atom yield from the C(^{1}D) + CH_4 reaction in the absence of competing H-atom losses. (Blue open squares) H-atom signal from the C(^{1}D) + H_2 reaction with [H_2] = 2.5 × 10^{14} cm^{-3}; (blue solid line) biexponential fit to the C(^{1}D) + H_2 datapoints; (blue dashed line) theoretical H-atom yield from the C(^{1}D) + H_2 reaction in the absence of competing H-atom losses.

Biexponential fits to these curves yielded values for the signal amplitude *A* of expression (1) which represents the theoretical H-atom yield in the absence of competing losses (see Figure 7 of Bourgalais et al.[33] for a similar analysis). To obtain the absolute H-atom yield for any

particular pair of curves, it was first necessary to correct the derived *A* factors to account for absorption losses of the VUV excitation and fluorescence intensities by residual gases in the chamber (notably for CH_4 or C_2H_6). This correction was estimated to be less than 3 % for CH_4 and 7 % for C_2H_6 over the entire temperature range. The adjusted temperature dependent H-atom yields are listed in Table 2 and displayed in Figure 5 and are seen to vary only slightly as a function of temperature.

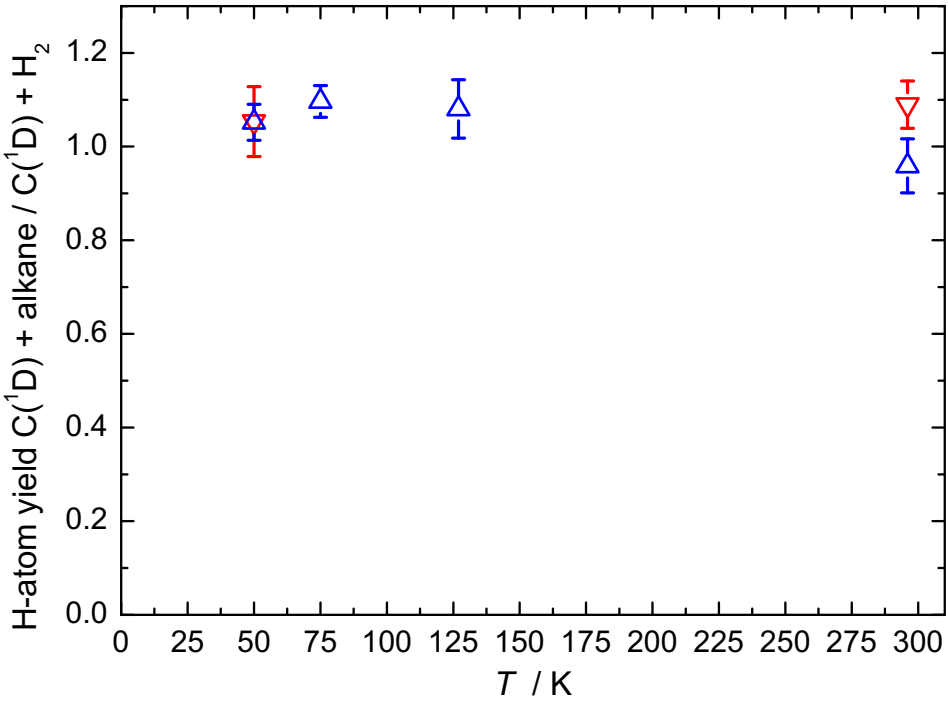

Figure 5 Temperature dependent product yields for the C(^{1}D) + alkane reactions. (Blue open triangles) H-atom yields for the C(^{1}D) + CH_4 reaction; (upside down red open triangles) H-atom yields for the C(^{1}D) + C_2H_6 reaction. Error bars represent statistical uncertainties at the 95 % confidence level.

Table 2 H-atom yields for the $C(^1D) + CH_4$ and $C(^1D) + C_2H_6$ reactions as a function of temperature

T / K	N[a]	H-atom yield $C(^1D) + CH_4$	N	H-atom yield $C(^1D) + C_2H_6$
296	12	0.96 ± 0.06[b]	9	1.09 ± 0.05
127	8	1.08 ± 0.06		
75	8	1.10 ± 0.03		
50	9	1.05 ± 0.04	2	1.05 ± 0.07

[a] Number of pairs of decay curves. [b]The error bars reflect the statistical uncertainties at the 95 % confidence level.

4 Discussion

It can be seen from Figure 3 that the room temperature value of the rate constant measured in the present work for the $C(^1D) + CH_4$ reaction is in excellent agreement with earlier work by Husain and Kirsch,[12] while the measured value of Braun et al.[34] is almost an order of magnitude lower. Leonori et al.[19] performed a combined experimental and theoretical investigation of the $C(^1D) + CH_4$ reaction using a crossed molecular beam apparatus alongside statistical calculations based on electronic structure calculations of the stationary points of the underlying singlet PES. The measurements were performed at a collision energy of 25.3 kJ mol^{-1} employing a universal mass spectrometric technique to detect the product species through tunable electron impact ionization. Experimentally, these authors attempted to detect signal at $m/z = 27$, corresponding to the C_2H_3 vinyl radical fragment channel (1c), which is expected to be the major H-atom elimination pathway. They were unable to observe any signal at $m/z = 27$, indicating that the products at this mass either (I) fell apart before reaching the detector (presumably yielding $C_2H_2/H_2CC + H$ as secondary products) or (II) underwent complete dissociative ionization. Given the use of low energy (17 eV) ionizing electrons in these preliminary experiments, Leonori et al.[19] favored the first scenario as the most likely one. Further evidence regarding the facile secondary dissociation of vinyl radicals has also been obtained by Lee et al. during their investigation of C_2H_4 photolysis.[35] To fit the $m/z = 26$ angular and time-of-flight distributions in the experiments of Leonori et al.[19] required the use of two

components, corresponding to the daughter ion of the vinyl radical channel (1c) in addition to the $C_2H_2/H_2CC + H_2$ product channels (1a) and (1b). From a consideration of these results, these authors determined a branching ratio of 0.8 ± 0.4 between H_2 and H loss pathways, a value which equates to 44 % H_2 elimination and 56 % H elimination. Considering that all the vinyl radicals produced in channel (1c) decompose to $C_2H_2/H_2CC + H$ at a collision energy of 25.3 kJ mol^{-1}, means that the H-atom yield from the $C(^1D) + CH_4$ reaction should be around 1.1, with two H-atoms being produced. This result compares well with our experimentally determined H-atom yields with an average value of 1.05 at much lower equivalent collision energies (< 3.7 kJ mol^{-1}) as shown in Figure 5 and listed in Table 2. The two sets of results are thus entirely consistent with the mechanism proposed by Leonori et al.[19]

Another important aspect of the $C(^1D) + CH_4$ system is the influence of non-adiabatic effects on the reaction mechanism and therefore on the overall reaction rate. Previous theoretical work by Kim et al.[10] has clearly identified a minimum on the seam of crossing between the $^1A'$ and $^3A''$ electronic states of C_2H_4 which could potentially play an important role in the reaction. In their work, the crossing point was found to be located in the vicinity of the $HCCH_3$ intermediate, formed by carbon atom insertion into a C-H bond of CH_4, with the singlet and triplet forms of $HCCH_3$ being almost isoenergetic. Indeed, the geometry of the minimum itself was very similar to that of $^1HCCH_3$. It is possible that the large rate constant increase we observe at low temperature could originate from these non-adiabatic effects. At higher temperature, reaction over the singlet surface is expected to dominate due to the shorter intermediate lifetimes. As the temperature falls, the lifetime of the $^1HCCH_3$ intermediate is expected to increase significantly, thereby promoting intersystem crossing to the triplet surface and providing an additional open pathway for reaction to occur. In this instance, Kim et al.[10] determined that the sole reaction products are $C_2H_3 + H$ over the triplet surface at low collision energies so that the formation of these products in addition to the $C_2H_2 + H_2$ and $C_2H_2/H_2CC +$

H + H pathways over the singlet surface should be reflected in our measured H-atom product branching ratios at low temperature. As shown in Figure 5, we obtain H-atom yields which increase very slightly as the temperature falls. If vinyl radicals produced in the triplet channel dissociate almost exclusively to C_2H_2/H_2CC + H (this would seem to be a reasonable assumption given the experimental evidence[19] that vinyl radicals formed over the singlet surface readily fall apart), the result should be the production of two hydrogen atoms for the formation of each $^3HCCH_3$ intermediate. As a large fraction of the singlet surface reaction leads to H_2 production, a small increase in the overall H-atom yield is expected if intersystem crossing becomes more important at low temperature. Further dynamical investigations of the $C(^1D)$ + CH_4 reaction at lower collision energies would be worthwhile in this respect to disentangle the relative contributions of these two surfaces to the overall reaction mechanism.

In the case of the $C(^1D)$ + C_2H_6 reaction, although no previous studies of this reaction could be found, we can refer to previous work on related systems such as C_3H_6 decomposition[21] and the $^1CH_2$ + C_2H_4 reaction[22-24] to help our interpretation of the H-atom yields obtained during this study. In particular, Hung et al.[21] performed a joint experimental and theoretical study of the thermal decomposition mechanism of propene in the range 1450-1712 K. They determined that of the several open pathways, the major product channels were likely to be H + C_3H_5 (85 %) and CH_3 + C_2H_3 (15 %) from RRKM calculations. Although the experimental H-atom yields measured using a shock tube apparatus were found to be in the range 1.7-2.0, (this value should be less than 1 if the major channels are those described above) they were nonetheless considered to be in agreement with the calculations as the C_3H_5 and C_2H_3 products were considered to undergo subsequent rapid thermal dissociation to produce secondary H-atoms.

Interestingly, the $^1CH_2$ + C_2H_4 reaction also occurs over the same singlet C_3H_6 surface. Gannon et al.[22, 23] measured product branching ratios for this reaction over the 195-498 K temperature range in two different studies, measuring H-atom yields which increased with

temperature from 0.35 - 1.08. Ye et al.[24] performed variable reaction coordinate transition state theory (VRC TST) calculations to determine branching ratios for the $^1CH_2 + C_2H_4$ reaction. In common with the studies of Hung et al.[21] and Gannon et al.[22, 23] they found that the major product channels were $H + C_3H_5$ and $CH_3 + C_2H_3$ in addition to C_3H_6 stabilization even at relatively low pressure (75 Torr) over the 300-2000 K range. In this case, the reagents $^1CH_2$ and C_2H_4 are ~ 460 kJ mol^{-1} higher in energy than C_3H_6; a value which can be compared with the one for $C(^1D) + C_2H_6$ of ~ 730 kJ mol^{-1} (also relative to C_3H_6). Given the lower pressure used and the high energy of the reagents with respect to C_3H_6, intermediate stabilization is likely to be very minor in the present work, so we need only consider bimolecular exit channels. It can be seen from Figure 5 that the H-atom yields determined in the present experiments are independent of temperature. Although our H-atom yields are smaller than those derived from the C_3H_6 thermal decomposition measurements of Hung et al.,[21] they are nonetheless in good agreement with the higher temperature experiments of Gannon et al.,[22] which might be expected given the considerable excess energy of the $C(^1D) + C_2H_6$ system compared to the $^1CH_2 + C_2H_4$ one. Moreover, as a yield slightly greater than 1 is obtained, these results also indicate that at least part of the products formed by the $C(^1D) + C_2H_6$ reaction fall apart to give secondary H-atoms. Indeed, as C_2H_3 radicals formed by the $C(^1D) + CH_4$ reaction were already considered to dissociate readily,[19] a similar outcome is likely here although perhaps less efficiently as the CH_3 cofragment is expected to carry away a significant fraction of the available excess energy.

The high measured values of the rate constant for the $C(^1D) + C_2H_6$ reaction (ranging from 4.6×10^{-10} cm^3 s^{-1} at 296 K to 3.3×10^{-10} cm^3 s^{-1} at 50 K) are consistent with reaction being dominated by long range forces, occurring at essentially every collision according to a capture type behavior. As neither of the reagents possess permanent dipole moments, reaction arises through dispersion interactions alone which depend on the polarizabilities of the individual species. As a result, in the absence of other factors, we would expect these dispersion

terms to yield a temperature dependent rate constant that is proportional to $T^{1/6}$.[36] Such a dependence is illustrated in Figure 3 by the solid red line and reproduces quite well the reactivity trend of the $C(^1D) + C_2H_6$ reaction. Future statistical (RRKM) type calculations would be very useful to provide a more precise interpretation of the $C(^1D) + C_2H_6$ system in terms of its overall reactivity and preferred product channels at low temperature.

5 Conclusions

The kinetics of the $C(^1D) + CH_4$ and $C(^1D) + C_2H_6$ reactions have been studied using a supersonic flow apparatus over the 50 – 296 K temperature range. In addition, absolute temperature dependent H-atom product yields have been measured for these processes over the same temperature range by comparison with the H-atom yield of the $C(^1D) + H_2$ reference reaction. The measured rate constants of the $C(^1D) + CH_4$ reaction are in good agreement with earlier measurements at room temperature. Nevertheless, the rate constant for this process displays a marked increase below 100 K, indicating a change in reaction mechanism at low temperature potentially brought about by intersystem crossing. The H-atom yield measurements agree well with earlier product studies of the $C(^1D) + CH_4$ reaction using a crossed molecular beam method at higher energy. The measured rate constants for the $C(^1D) + C_2H_6$ reaction display a distinctly different temperature dependence to the $C(^1D) + CH_4$ ones, following a capture type rate law giving rise to a positive temperature dependence. Although no previous measurements exist of the $C(^1D) + C_2H_6$ reaction, comparison with previous work over the singlet C_3H_6 potential energy surface provides a consistent interpretation of the measured H-atom yields, indicating that the major product channels are likely to be $C_3H_5 + H$ and $C_2H_3 + CH_3$.

Supporting Information

Figure S1. Product H-atom formation curves for the $C(^1D) + CH_4$ reaction recorded at 50 K in the presence and absence of excess N_2.

Acknowledgements

K.M.H. and D.N.R acknowledge support from the French program "Physique et Chimie du Milieu Interstellaire" (PCMI) funded by the Conseil National de la Recherche Scientifique (CNRS) and Centre National d'Etudes Spatiales (CNES).

References

1. Anders, E.; Grevesse, N. Abundances of the Elements: Meteoritic and Solar. *Geochimica et Cosmochimica Acta* **1989,** *53*, 197-214.
2. Baulch, D. L.; Bowman, C. T.; Cobos, C. J.; Cox, R. A.; Just, Th.; Kerr, J. A.; Pilling, M. J.; Stocker, D.; Troe, J.; Tsang, W. et al. Evaluated Kinetic Data for Combustion Modeling: Supplement II. *J. Phys. Chem. Ref. Data* **2005,** *34*, 757-1397.
3. Dobrijevic, M.; Hebrard, E.; Loison, J. C.; Hickson, K. M. Coupling of Oxygen, Nitrogen, and Hydrocarbon Species in the Photochemistry of Titan's Atmosphere. *Icarus,* **2014**, *228*, 324–346.
4. Loison, J. C.; Wakelam, V.; Hickson, K. M.; Bergeat, A.; Mereau, R. The Gas-Phase Chemistry of Carbon Chains in Dark Cloud Chemical Models. *Mon. Not. R. Astron. Soc*. **2014,** *437*, 930-945.
5. Chastaing, D.; James, P. L.; Sims, I. R.; Smith, I. W. M. Neutral-Neutral Reactions at the Temperatures of Interstellar Clouds: Rate Coefficients for Reactions of Atomic Carbon, $C(^3P)$, with O_2, C_2H_2, C_2H_4 and C_3H_6 down to 15 K. *Phys. Chem. Chem. Phys.* **1999,** *1*, 2247-2256.
6. Chastaing, D.; Le Picard, S. D.; Sims, I. R.; Smith, I. W. M. Rate Coefficients for the Reactions of $C(^3P_j)$ Atoms with C_2H_2, C_2H_4, CH_3CCH and $H_2C=C=CH_2$ at Temperatures down to 15 K. *Astron. Astrophys.* **2001,** *365*, 241-247.
7. Costes, M.; Halvick, P.; Hickson, K. M.; Daugey, N.; Naulin, C. Non-Threshold, Threshold, and Nonadiabatic Behavior of the Key Interstellar $C + C_2H_2$ reaction. *Astrophys. J.* **2009,** *703*, 1179-1187.
8. Leonori, F.; Petrucci, R.; Segoloni, E.; Bergeat, A.; Hickson, K. M.; Balucani, N.; Casavecchia, P. Unraveling the Dynamics of the $C(^3P,^1D) + C_2H_2$ Reactions by the Crossed Molecular Beam Scattering Technique. *J. Phys. Chem. A* **2008,** *112*, 1363-1379.
9. Hickson, K. M.; Loison, J.-C.; Wakelam, V. Temperature Dependent Product Yields for the Spin Forbidden Singlet Channel of the $C(^3P) + C_2H_2$ Reaction. *Chem. Phys. Lett.* **2016,** *659*, 70-75.
10. Kim, G. S.; Nguyen, T. L.; Mebel, A. M.; Lin, S. H.; Nguyen, M. T. Ab Initio/RRKM Study of the Potential Energy Surface of Triplet Ethylene and Product Branching Ratios of the $C(^3P) + CH_4$ Reaction. *J. Phys. Chem. A* **2003,** *107*, 1788-1796.
11. Blint, R. J.; Newton, M. D. Ab Initio Potential Energy Surfaces for the Reactions of Atomic Carbon with Molecular Hydrogen. *Chem. Phys. Lett.* **1975,** *32*, 178-183.

12. Husain, D.; Kirsch, L. J. Study of Electronically Excited Carbon Atoms, $C(2^1D_2)$, by Time-Resolved Atomic Absorption at 193.1 nm, ($3^1P_1°$-2^1D_2) .2. Reactions of $C(2^1D_2)$ with Molecules. *Transactions of the Faraday Society* **1971,** *67*, 3166-3175.
13. Kaiser, R. I.; Nguyen, T. L.; Mebel, A. M.; Lee, Y. T. Stripping Dynamics in the Reactions of Electronically Excited Carbon Atoms, $C(^1D)$, with Ethylene and Propylene-Production of Propargyl and Methylpropargyl Radicals. *J. Chem. Phys.* **2002,** *116*, 1318-1324.
14. Husain, D.; Kirsch, L. J. The Study of Electronically Excited Carbon Atoms, $C(2^1D_2)$, by Photoelectric Measurement of Time-Resolved Atomic Absorption. *Chem. Phys. Lett.* **1971,** *9*, 412-415.
15. Fisher, W. H.; Carrington, T.; Sadowski, C. M.; Dugan, C. H. The Reactions of $C(2^1D_2)$ with H_2, D_2 and HD: Product Rotational Energies, Isotope Effects and the CD/CH Branching Ratio. *Chem. Phys.* **1985,** *97*, 433-448.
16. Sato, K.; Ishida, N.; Kurakata, T.; Iwasaki, A.; Tsnuashima, S. Reactions of $C(^1D)$ with H_2 , HD and D_2 : Kinetic Isotope Effect and the CD/CH Branching Ratio. *Chem. Phys.* **1998,** *237*, 195-204.
17. Hickson, K. M.; Loison, J. C.; Guo, H.; Suleimanov, Y. V. Ring-Polymer Molecular Dynamics for the Prediction of Low-Temperature Rates: An Investigation of the $C(^1D) + H_2$ Reaction. *J. Phys. Chem. Lett.* **2015,** *6*, 4194-4199.
18. Hickson, K. M.; Suleimanov, Y. V. An Experimental and Theoretical Investigation of the $C(^1D) + D_2$ Reaction. *Phys. Chem. Chem. Phys.* **2017,** *19*, 480-486.
19. Leonori, F.; Skouteris, D.; Petrucci, R.; Casavecchia, P.; Rosi, M.; Balucani, N. Combined Crossed Beam and Theoretical Studies of the $C(^1D) + CH_4$ Reaction. *J. Chem. Phys.* **2013,** *138*, 024311.
20. Stoliarov, S. I.; Knyazev, V. D.; Slagle, I. R. Experimental Study of the Reaction between Vinyl and Methyl Radicals in the Gas Phase. Temperature and Pressure Dependence of Overall Rate Constants and Product Yields. *J. Phys. Chem. A* **2000,** *104*, 9687-9697.
21. Hung, W.-C.; Tsai, C.-Y.; Matsui, H.; Wang, N.-S.; Miyoshi, A. Experimental and Theoretical Study on the Thermal Decomposition of C_3H_6 (Propene). *J. Phys. Chem. A* **2015,** *119*, 1229-1237.
22. Gannon, K. L.; Blitz, M. A.; Liang, C. H.; Pilling, M. J.; Seakins, P. W.; Glowacki, D. R. Temperature Dependent Kinetics (195−798 K) and H Atom Yields (298−498 K) from Reactions of $^1CH_2$ with Acetylene, Ethene, and Propene. *J. Phys. Chem. A* **2010,** *114*, 9413-9424.
23. Gannon, K. L.; Blitz, M. A.; Liang, C. H.; Pilling, M. J.; Seakins, P. W.; Glowacki, D. R.; Harvey, J. N. An Experimental and Theoretical Investigation of the Competition between Chemical Reaction and Relaxation for the Reactions of $^1CH_2$ with Acetylene and Ethene: Implications for the Chemistry of the Giant Planets. *Faraday Discuss*. **2010**, *147*, 1-16.
24. Ye, L.; Georgievskii, Y.; Klippenstein, S. J. Pressure-Dependent Branching in the Reaction of $^1CH_2$ with C_2H_4 and Other Reactions on the C_3H_6 Potential Energy Surface. *Proc. Combust. Inst.* **2015,** *35*, 223-230.
25. Hébrard, E.; Dobrijevic, M.; Loison, J. C.; Bergeat, A.; Hickson, K. M.; Caralp, F. Photochemistry of C_3H_p Hydrocarbons in Titan's Stratosphere Revisited. *Astron. Astrophys.* **2013,** *552*, A132.
26. Daugey, N.; Caubet, P.; Retail, B.; Costes, M.; Bergeat, A.; Dorthe, G. Kinetic Measurements on Methylidyne Radical Reactions with Several Hydrocarbons at Low Temperatures. *Phys. Chem. Chem. Phys.* **2005,** *7*, 2921-2927.
27. Daugey, N.; Caubet, P.; Bergeat, A.; Costes, M.; Hickson, K. M. Reaction Kinetics to Low Temperatures. Dicarbon + Acetylene, Methylacetylene, Allene and Propene from $77 \leq T \leq 296$ K. *Phys. Chem. Chem. Phys.* **2008,** *10*, 729-737.

28. Hickson, K. M.; Loison, J.-C.; Lique, F.; Kłos, J. An Experimental and Theoretical Investigation of the $C(^1D) + N_2 \rightarrow C(^3P) + N_2$ Quenching Reaction at Low Temperature. *J. Phys. Chem. A* **2016,** *120*, 2504-2513.
29. Grondin, R.; Loison, J.-C.; Hickson, K. M. Low Temperature Rate Constants for the Reactions of $O(^1D)$ with N_2, O_2, and Ar. *J. Phys. Chem. A* **2016,** *120*, 4838-4844.
30. Shannon, R. J.; Cossou, C.; Loison, J.-C.; Caubet, P.; Balucani, N.; Seakins, P. W.; Wakelam, V.; Hickson, K. M. The Fast $C(^3P) + CH_3OH$ Reaction as an Efficient Loss Process for Gas-Phase Interstellar Methanol. *RSC Advances* **2014,** *4*, 26342-26353.
31. Hickson, K. M.; Loison, J.-C.; Bourgalais, J.; Capron, M.; Picard, S. D. L.; Goulay, F.; Wakelam, V. The $C(^3P) + NH_3$ Reaction in Interstellar Chemistry. II. Low Temperature Rate Constants and Modeling of NH, NH_2, and NH_3 Abundances in Dense Interstellar Clouds. *Astrophys. J.* **2015,** *812*, 107.
32. Hickson, K. M.; Loison, J.-C.; Nuñez-Reyes, D.; Méreau, R. Quantum Tunneling Enhancement of the $C + H_2O$ and $C + D_2O$ Reactions at Low Temperature. *J. Phys. Chem. Lett.* **2016**, 3641-3646.
33. Bourgalais, J.; Capron, M.; Kailasanathan, R. K. A.; Osborn, D., L. ; Hickson, K., M.; Loison, J.-C.; Wakelam, V.; Goulay, F.; Le Picard, S. D. The $C(^3P) + NH_3$ Reaction in Interstellar Chemistry. I. Investigation of the Product Formation Channels. *Astrophys. J.* **2015,** *812*, 106.
34. Braun, W.; Bass, A. M.; Davis, D. D.; Simmons, J. D. Flash Photolysis of Carbon Suboxide: Absolute Rate Constants for Reactions of $C(^3P)$ and $C(^1D)$ with H_2, N_2, CO, NO, O_2 and CH_4. *Proc. Roy. Soc. A* **1969,** *312*, 417-434.
35. Lee, S. H.; Lee, Y. T.; Yang, X. Dynamics of Photodissociation of Ethylene and its Isotopomers at 157 nm: Branching Ratios and Kinetic-Energy Distributions. *J. Chem. Phys.* **2004,** *120*, 10983-10991.
36. Georgievskii, Y.; Klippenstein, S. J. Long-Range Transition State Theory. *J. Chem. Phys.* **2005,** *122*, 194103-194117.

TOC Graphic

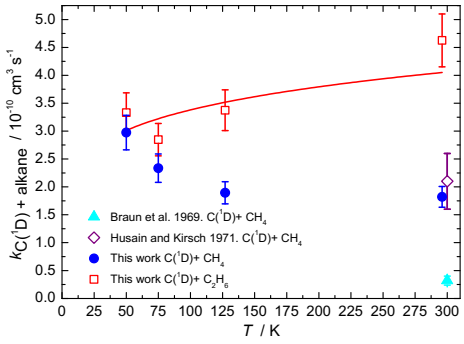
$k_{C(^1D)+alkane}$ / 10^{-10} cm^3 s^{-1}
T / K
Braun et al. 1969. C(1D)+ CH4
Husain and Kirsch 1971. C(1D)+ CH4
This work C(1D)+ CH4
This work C(1D)+ C2H6